View metadata, citation and similar papers at core.ac.uk
brought to you by CORE
provided by Elsevier - Publisher Connector

Cell, Vol. 122, 579–591, August 26, 2005, Copyright ©2005 by Elsevier Inc. DOI 10.1016/j.cell.2005.06.022

A Role for Proapoptotic BID in the DNA-Damage Response

Sandra S. Zinkel,[1,3,4,*] Kristen E. Hurov,[1,3] Christy Ong,[1] Farvardean M. Abtahi,[1] Atan Gross,[2] and Stanley J. Korsmeyer[1]
[1]Howard Hughes Medical Institute
Dana-Farber Cancer Institute
Harvard Medical School
Boston, Massachusetts 02115
[2]Department of Biological Regulation
Weizmann Institute of Science
Rehovot 7610
Israel

Summary

The BCL-2 family of apoptotic proteins encompasses key regulators proximal to irreversible cell damage. The BH3-only members of this family act as sentinels, interconnecting specific death signals to the core apoptotic pathway. Our previous data demonstrated a role for BH3-only BID in maintaining myeloid homeostasis and suppressing leukemogenesis. In the absence of *Bid*, mice accumulate chromosomal aberrations and develop a fatal myeloproliferative disorder resembling chronic myelomonocytic leukemia. Here, we describe a role for BID in preserving genomic integrity that places BID at an early point in the path to determine the fate of a cell. We show that BID plays an unexpected role in the intra-S phase checkpoint downstream of DNA damage distinct from its proapoptotic function. We further demonstrate that this role is mediated through BID phosphorylation by the DNA-damage kinase ATM. These results establish a link between proapoptotic *Bid* and the DNA-damage response.

Introduction

The BCL-2 family of proteins is predominantly situated upstream of irreversible cellular damage in the intrinsic apoptotic pathway (reviewed in Danial and Korsmeyer [2004]). Pro- as well as antiapoptotic members contribute to apoptotic susceptibility and the predisposition to cancer. The BH3-only proapoptotic members connect specific proximal death signals with the multidomain proapoptotic molecules BAX and BAK that serve as an obligate gateway to apoptotic death. The multidomain antiapoptotic members bind and sequester BH3-only molecules to protect from activation of BAX, BAK as one mechanism of preventing death.

The BH3-only member BID serves the unique function of interconnecting the extrinsic death receptors for TNFα and Fas to the mitochondrial amplification loop of the intrinsic pathway. In a resting cell, BID is predominantly cytoplasmic. Following TNFα or Fas treatment, BID is cleaved by caspase 8 in an unstructured loop, exposing a new amino terminal glycine residue, which becomes myristoylated, facilitating its translocation to the mitochondria (Zha et al., 2000). Activated BH3-only proteins such as caspase-truncated BID (tBID) either directly or indirectly activate BAX and BAK, which are required for the release of cytochrome c and the downstream apoptotic program.

Mouse embryonic fibroblasts (MEFs) doubly deficient in BAX and BAK are resistant to apoptosis induced by treatment with DNA-damaging agents, such as etoposide and ultraviolet (UV) irradiation (Wei et al., 2001). Several BH3-only proteins, namely *Noxa* and *Puma* have been implicated as upstream regulators of DNA damage-induced apoptosis. *Noxa* responds to p53-dependent apoptosis following etoposide and UV-induced DNA damage. *Noxa*-deficient intestinal crypt cells but not thymocytes are resistant to high doses of ionizing radiation (IR; Shibue et al., 2003). *Puma* plays a role in thymocyte apoptosis following IR and etoposide treatments (Villunger et al., 2003).

The role of BID in normal development and cellular homeostasis has been characterized using mice in which *Bid* has been disrupted. When challenged with lethal doses of agonistic anti-Fas antibody, mice without BID are resistant to the ensuing Fas-induced hepatocellular apoptosis, indicating a critical role for a BID-dependent mitochondrial amplification loop in this liver cell death (Yin et al., 1999). Despite this dramatic phenotype, $Bid^{-/-}$ mice successfully complete embryonic development and their livers appear grossly normal. However, as they age, $Bid^{-/-}$ mice spontaneously develop a myeloproliferative disorder that progresses to a fatal disease resembling chronic myelomonocytic leukemia (CMML). This indicates an essential role for BID in maintaining myeloid homeostasis and suppressing leukemogenesis (Zinkel et al., 2003).

A critical question is how BID is involved in suppressing oncogenesis. While the loss of BID could theoretically reset death susceptibility in both intrinsic and extrinsic pathways, it is less obvious why the absence of BID should prove so oncogenic. A striking feature of the BID-deficient CMML is the frequent presence of genomic instability as evidenced by chromosomal translocation (Zinkel et al., 2003). This suggests that BID might also serve a role in preserving genomic integrity.

Progression to malignancy is a multistep process in which a succession of genetic changes culminates in phenotypic changes (Jacks and Weinberg, 2002). Maintenance of genomic integrity is of fundamental importance to the survival and health of an organism. DNA is highly reactive and subject to damage by multiple reagents including reactive oxygen species, methylating agents, both UV and IR as well as stochastic errors that can arise during DNA replication and recombina-

*Correspondence: sandra.zinkel@vanderbilt.edu
[3]These authors contributed equally to this work.
[4]Present address: Department of Medicine, Vanderbilt University School of Medicine, Vanderbilt-Ingram Cancer Center, Nashville, Tennessee 37232.

tion. Cells respond to the presence of DNA damage by activating cell cycle checkpoints and repair mechanisms, and ultimately the damaged cell is eliminated through apoptosis.

The cellular response to DNA damage varies by cell type. For example, fibroblasts are relatively resistant to DNA damage-induced apoptosis; they prevent proliferation of mutations by entering into long-term G1 or G2 arrest (Baus et al., 2003; Di Leonardo et al., 1994). Hematopoietic cells are primed to undergo apoptosis following treatment with DNA-damaging agents. The signals that govern whether a cell initiates DNA repair, enters cell cycle arrest, or undergoes apoptosis and the means by which the cell integrates information from these pathways are not yet understood. Three DNA repair kinases have been identified. ATM (Ataxia-telangiectasia mutated), ATR (ATM and RAD3-related) and DNA-PK (reviewed in Sancar et al. [2004]). The specific DNA-damage signals that activate ATM or ATR are not well defined in part due to the multiple distinct DNA lesions generated by signals such as IR, UV, and alkylating agents (Nyberg et al., 2002). ATM has been reported to respond primarily to agents such as IR that generate double-strand breaks, while ATR appears to respond to agents inducing multiple types of DNA damage (Zhou and Elledge, 2000). Fibroblasts deficient in ATM demonstrate increased sensitivity to IR but not to UV, alkylating agents, or inhibitors of DNA replication (Banin et al., 1998; Canman et al., 1998; Zhou and Elledge, 2000). Cells expressing kinase-inactive ATR demonstrate increased sensitivity to IR, UV, cisplatin, and methyl methane sulfonate (Cliby et al., 1998). ATR is required for cell cycle regulation and phosphorylation of downstream kinases such as Chk1 in response to replication blocks and UV irradiation (Guo et al., 2000). Both ATM and ATR relocalize to nuclear foci following DNA damage (Andegeko et al., 2001; Tibbetts et al., 2000), and both kinases display a common substrate preference (Kim et al., 1999; Manke et al., 2003; O'Neill et al., 2000).

Bid$^{-/-}$ primary MEFs have been shown to be somewhat resistant to chemotherapeutic drugs 5-fluorouracil (5-FU) and adriamycin (Sax et al., 2002), but not to UVC or etoposide (Wei et al., 2001). Thus, BID does not appear to play a prominent role in the apoptotic response downstream of DNA damage in fibroblasts. However, *Bid*$^{-/-}$ mice progress to a high incidence of myeloid malignancy with considerable genomic instability in that cell type. Wild-type hematopoietic cells have a marked propensity for apoptosis in response to DNA damage; yet in the absence of BID, myeloid cells accumulate mutations, resist apoptosis, and display aspects of unchecked proliferation. This suggests that BID may itself play a role in DNA repair, in cell cycle checkpoint response, or in integrating apoptosis and the DNA repair response. In this study, we describe a novel role for BID in preserving genomic integrity that places BID at an early point in the path to determine the fate of a cell. We show that BID plays an unexpected role in the intra-S phase checkpoint downstream of DNA damage. We further demonstrate that this role is mediated through BID phosphorylation by the DNA-damage kinase ATM.

Results

Bid$^{-/-}$ Myeloid Progenitor Cells (MPCs) Display Increased "Chromatid Type" Chromosomal Instability Following Mitomycin C Treatment

Bid-deficient CMMLs are clonal and display chromosomal aberrations. SKY analysis of the *Bid*$^{-/-}$ leukemia revealed chromosomal translocations and duplications (Zinkel et al., 2003). In addition, array CGH studies of multiple tumors revealed recurrent sites of chromosomal amplification (data not shown). Absence of proapoptotic BID may enable the accumulation of cells with genetic lesions and foster their survival. Alternatively, genomic instability may be intrinsic to *Bid*$^{-/-}$ cells, implicating a role for BID in a DNA-damage pathway. To investigate the function of BID in myeloid cells, we generated *Hox11*-immortalized premalignant myeloid progenitor cell lines (MPCs) from *Bid*$^{+/+}$ and *Bid*$^{-/-}$ genotypes. Doses of mitomycin c that had little effect on *Bid*$^{+/+}$ MPCs displayed a marked increase in chromosomal instability in *Bid*$^{-/-}$ MPCs. Of note, metaphase spreads from mitomycin c-treated *Bid*$^{-/-}$ MPCs displayed tri- and quadriradial chromosomal figures (Figure 1A), quantifiable by an increase in the number of breaks per cell (Figure 1B). These abnormal chromosomal structures represent "chromatid type" errors resulting from improperly repaired DNA damage accrued during S phase of the cell cycle (Scully et al., 2000) and are characteristic of cells with a defect in DNA repair, such as those in Fanconi anemia (D'Andrea, 2003), Bloom's syndrome (Langland et al., 2002; Wu et al., 2001), and the hereditary breast and ovarian cancer syndromes involving BRCA1 (Scully and Livingston, 2000). Activated peripheral T cells isolated from *Bid*$^{-/-}$ mice also display increased chromosomal instability following mitomycin c treatment (Figures 1C and 1D), indicating that this increased chromosomal instability is a general feature of *Bid* deficiency, although it is more pronounced in myeloid cells.

Bid$^{-/-}$ MPCs Display Increased Sensitivity to DNA-Damaging Agents

Cells defective in DNA repair exhibit increased sensitivity to DNA-damaging agents (D'Andrea, 2003; Frei and Gasser, 2000; Stewart et al., 1997). Following treatment with hydroxyurea or mitomycin c, agents that induce DNA damage through replicative stress, *Hox11*-immortalized *Bid*$^{-/-}$ MPCs, display increased cell death (Figure 2A). *Bid*$^{-/-}$ primary MPCs (see Figure S1 in the Supplemental Data available with this article online) and *Bid*$^{-/-}$ primary activated T cells (Figures 2B and 2C) display similarly increased mitomycin c sensitivity, confirming that the increased death response to replicative stress is not due to *Hox11* immortalization and is a general feature of *Bid* deficiency. In contrast, there was no significant difference in viability in response to treatment with UV or IR; treatment with etoposide, an inhibitor of topoisomerase 2, resulted in a modest protection of *Bid*$^{-/-}$ MPCs from apoptosis (Figure 2A). Hydroxyurea washout experiments also revealed decreased viability of *Bid*$^{-/-}$ MPCs relative to *Bid*$^{+/+}$ MPCs (Figure 2B). Interestingly, we find a small but significant de-

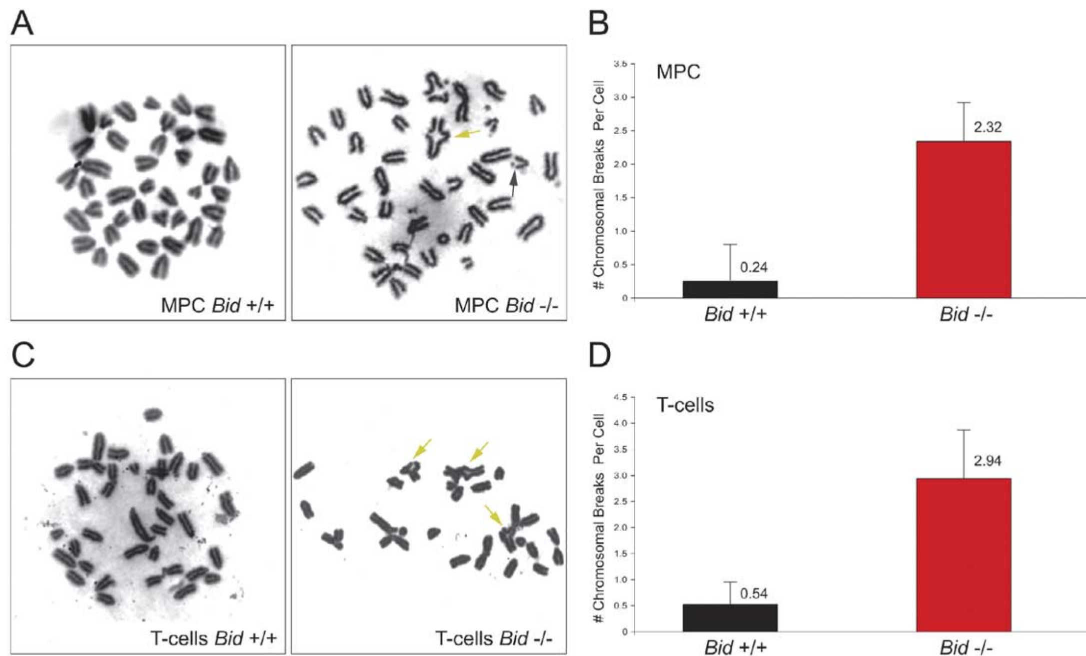

Figure 1. *Bid*$^{-/-}$ Cells Demonstrate Increased Chromosomal Damage in Response to Mitomycin C Treatment

The error bars represent the standard deviation of the data obtained from 50 metaphase spreads.

(A) Metaphase spreads of wild-type and *Bid*$^{-/-}$ MPCs after 24 hr of treatment with mitomycin c (100 nM). Cells were arrested in metaphase with 0.1 mg/ml of colchicine, fixed, and visualized by Giemsa staining. The yellow arrow designates a quadriradial, and the black arrow designates a chromosomal break.

(B) Quantification of the number of chromosomal breaks per cell evaluated in 50 metaphase spreads.

(C) Metaphase spreads of wild-type and *Bid*$^{-/-}$ primary activated T cells after 24 hr of treatment with mitomycin c (100 nM). Cells and chromosomes were prepared as in (A).

(D) Quantification of the number of chromosomal breaks per cell evaluated in 50 metaphase spreads.

crease in cell viability of *Bid*$^{-/-}$ primary activated T cells in response to IR (data not shown), a cell type that is less dependent upon the BID-mediated mitochondrial amplification loop for death (Scaffidi et al., 1998). The above data demonstrate a surprising sensitivity of cells deficient for proapoptotic BID in response to agents inducing DNA damage through replicative stress, suggesting a possible role for BID in this pathway that is distinct from its proapoptotic role.

BID$^{-/-}$ MPCs Fail to Accumulate in S Phase Following Replicative Stress

We next examined the cell cycle status of MPCs to characterize the role of *Bid* following replicative stress. As evidenced by propidium iodide staining, untreated *Bid*$^{+/+}$ and *Bid*$^{-/-}$ MPCs display an identical cell cycle profile. Following treatment with aphidicolin, *Bid*$^{+/+}$ MPCs but not *Bid*$^{-/-}$ MPCs arrest and accumulate in S phase (Figures 3Aa and 3Ab), suggesting either a defect in an S phase checkpoint, a failure of *Bid*$^{-/-}$ MPCs to progress from G1 to S phase, or death of *Bid*$^{-/-}$ MPCs in S phase. The increase in *Bid*$^{-/-}$ cells possessing <2N DNA content following aphidicolin treatment (Figure 3A) suggests that these *Bid*$^{-/-}$ cells undergo increased apoptosis. The percentage of cells in S phase from multiple independent experiments is presented in Figure S3. To further investigate the fate of S phase cells following replicative stress, we labeled S phase cells with BrDU immediately prior to treatment with hydroxyurea, (see Figure S4 for a schematic of the experimental design). After 2 hr of hydroxyurea treatment, cells were washed, and cell cycle progression of BrDU-positive cells was monitored by flow cytometry. The data point at time T0 was taken at the time of hydroxyurea washout, and the gates indicate early S phase and late S/G2 as cells initially in G1 are not labeled with BrDU and thus are not included in the analysis. Immediately following hydroxyurea treatment, BrDU^{+} cells from *Bid*$^{+/+}$ and *Bid*$^{-/-}$ display a similar cell cycle distribution (Figure 3B). By contrast, while at 6 hr *Bid*$^{+/+}$ cells display some progression from early to late S phase, *Bid*$^{-/-}$ cells display a significant decrease in the number of cells in late S phase, along with an increase in cells with <2N DNA content. These data are consistent either with increased progression of *Bid*$^{-/-}$ cells through S phase relative to *Bid*$^{+/+}$ cells, or increased death of *Bid*$^{-/-}$ cells in S phase. Taken together with the increased death seen in *Bid*$^{-/-}$ primary T cells at 6 hr after hydroxyurea treatment (Figure 2B), these data are consistent with death of *Bid*$^{-/-}$ cells progressing through S phase.

To verify that this S phase phenotype is attributable to the absence of BID, we stably transduced *Bid*$^{-/-}$

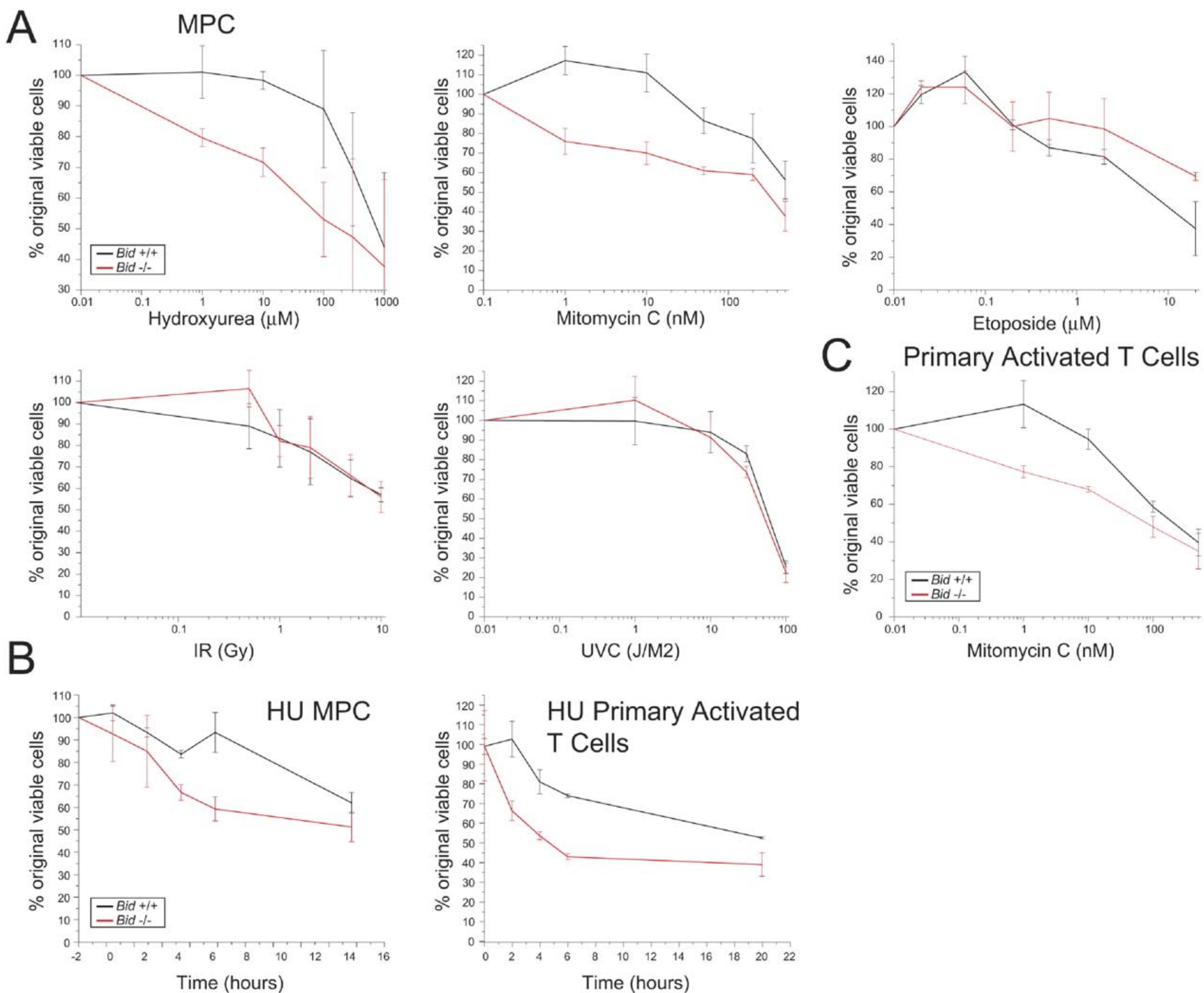

Figure 2. *Bid*$^{-/-}$ Cells Display Increased Sensitivity to DNA-Damage Agents

BID functions downstream of specific DNA-damage signals in MPCs. The error bars represent the standard deviation of data points from three independent experiments.

(A) Dose-response/survival curves of *Bid*$^{-/-}$ MPCs in response to stimuli inducing DNA damage and replicative stress. Wild-type and *Bid*$^{-/-}$ MPCs were evaluated for survival by Trypan blue exclusion following 24 hr of treatment with the indicated doses of hydroxyurea, mitomycin c, ultraviolet light, ionizing radiation, and etoposide.

(B) Panel 1: time course of survival of *Bid*$^{+/+}$ and *Bid*$^{-/-}$ MPCs treated for 2 hr with 200 μM hydroxyurea. Cells were washed and evaluated for survival by Trypan blue exclusion at the indicated time points. Panel 2: time course of survival of *Bid*$^{+/+}$ and *Bid*$^{-/-}$ activated T cells treated for two hours with 200 μM hydroxyurea. Cells were washed and evaluated as above. The percentage of antigen-specific activated CD8^{+} T cells in the cultures at the time of analysis is indicated in Figure S2.

(C) Dose-response/survival curves of *Bid*$^{+/+}$ and *Bid*$^{-/-}$ activated T cells following mitomycin c treatment at the indicated doses as in (A).

MPCs with recombinant retrovirus (Figure 3D). When wild-type BID is reexpressed at the endogenous level, cells accumulate at S phase following aphidicolin treatment (Figure 3C), confirming that the absence of BID is the cause of the S phase defect in *Bid*$^{-/-}$ MPCs.

A Functional BID BH3-Domain Is Not Required to Rescue S Phase Accumulation

The death function of proapoptotic BCL-2 family members is localized to the BH3 domain. To determine whether an intact BH3 domain is required for the BID-deficient S phase defect, *Bid*$^{-/-}$ MPCs were transduced with BID harboring various apoptosis-inactivating mutations in the BH3 domain. (Wang et al., 1996) Surprisingly, expression of endogenous levels of BID with mutant BH3 domains restores S phase accumulation of *Bid*$^{-/-}$ MPCs following aphidicolin treatment (Figures 4A and 4C). Furthermore, expression of either wild-type BID or BID with mutant BH3 domains protects *Bid*$^{-/-}$ MPCs from death in response to mitomycin c treatment, at a level comparable to that seen in *Bid*$^{+/+}$ MPCs (Figure 4B). Therefore, a region of BID distinct from its proapoptotic BH3 domain mediates the BID's role downstream of DNA damage induced by replicative stress.

BID Localizes to the Nucleus Following DNA Damage

Since signaling proteins involved in cell cycle checkpoints or DNA-damage response often function in the

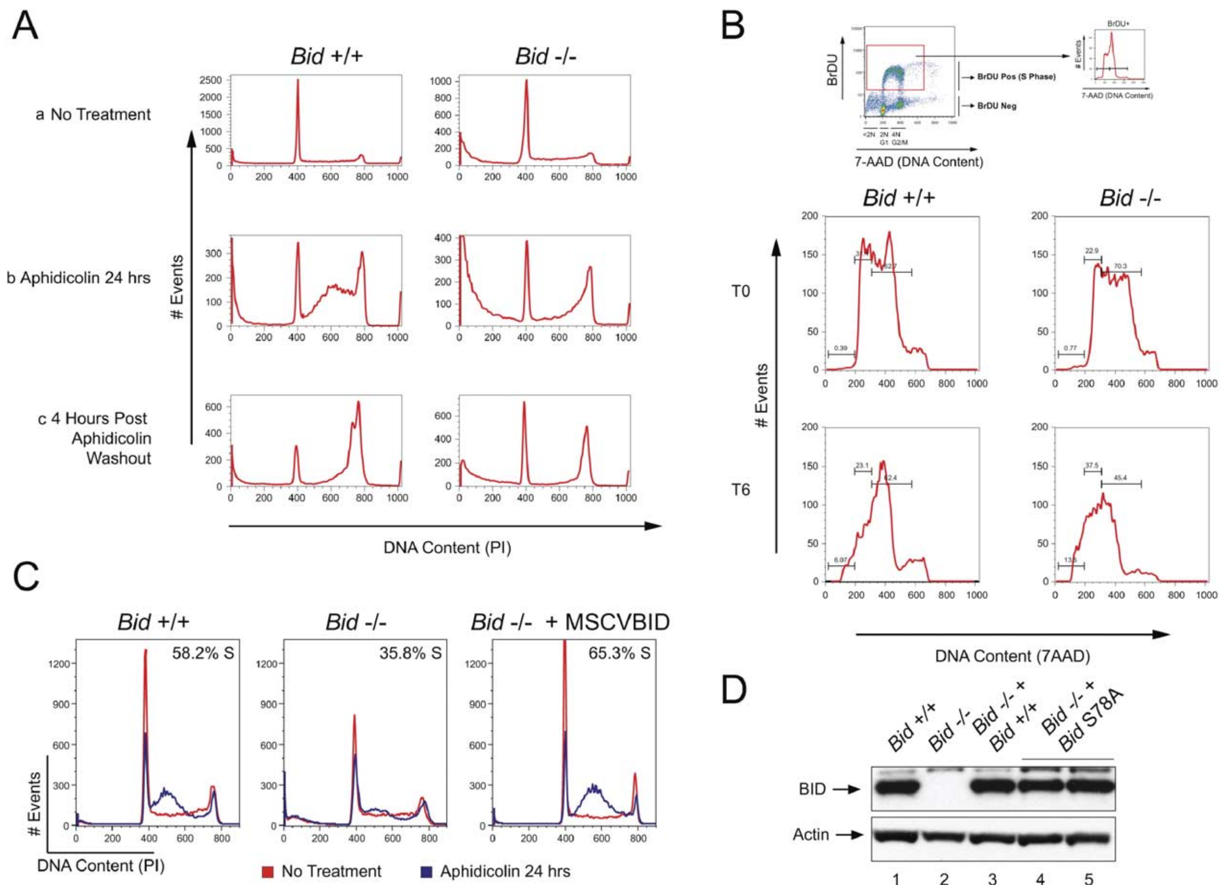

Figure 3. *Bid*$^{-/-}$ MPCs Fail to Accumulate in S Phase Following Treatment with Aphidicolin, Suggesting Defects in the S Phase Checkpoint

(A) Cell cycle analysis (propidium iodide staining) of *Bid*$^{+/+}$ and *Bid*$^{-/-}$ MPCs was compared in cells left untreated or following 18–24 hr of treatment with aphidicolin (0.1 μM).

(B) Increased death of S phase cells in *Bid*$^{-/-}$-activated T cells treated with hydroxyurea. *Bid*$^{+/+}$ and *Bid*$^{-/-}$ S phase cells were labeled with BrDU for 45 min (Figure S4). After 2 hr of hydroxyurea treatment, cells were washed, and progression of BrDU-positive cells through the cell cycle was monitored by flow cytometry (top panel indicates the gating used for analysis). The data point at time T0 was taken at the time of hydroxyurea washout, and the gates indicate early S phase and late S/G2. Cells initially in G1 are not labeled with BrDU and thus are not included in the analysis.

(C) Reintroduction of wild-type BID by retroviral transduction restores the ability of MPCs to accumulate in S phase following aphidicolin treatment.

(D) Reintroduction of wild-type *Bid* protein in *Bid*$^{-/-}$ MPCs via MSCVBID retroviral transduction results in expression similar to endogenous levels.

nucleus, we evaluated the subcellular localization of BID. Following treatment of wild-type MEFs with hydroxyurea or etoposide, BID localizes to the nuclei in the majority of cells (Figure 5A). Following IR treatment, BID is seen both in the nuclei and in the mitochondria (Figure 5A). Interestingly, nuclear BID is seen in approximately 14% of untreated cells, perhaps suggesting a role for *Bid* in the normal cell cycle. Although the level of tagged BID protein seen by Western blot analysis is modestly increased relative to endogenous BID levels in MEFs, there is no increase following treatment with DNA-damaging agents (Figure S5), suggesting that BID's change in subcellular localization cannot be accounted for by a change in protein level. Furthermore, subcellular fractionation of endogenous levels of BID in MPCs demonstrates an increase in BID primarily in the chromatin fraction of the nucleus following hydroxyurea treatment (Figure 5C). The apparent discrepancy in the percentage of nuclear BID after damage observed in subcellular fractionation versus immunofluorescence may be due to suboptimal recovery of BID from chromatin or loss of nuclear BID to the cytosolic fraction during fractionation. The distinct subcellular localization of BID following DNA damage suggests that the distinct functions for BID may be regulated at least in part by BID's location in the cell.

BID Is Phosphorylated Following Treatment with DNA-Damaging Agents

ATM, ATR, and DNA-PKcs (DNA-dependent protein kinase) are known to be involved in the DNA repair pathway (Reviewed in Sancar et al. [2004]). All three kinases display a substrate preference for serine or threonine followed by glutamine in a +1 position (Kim et al., 1999;

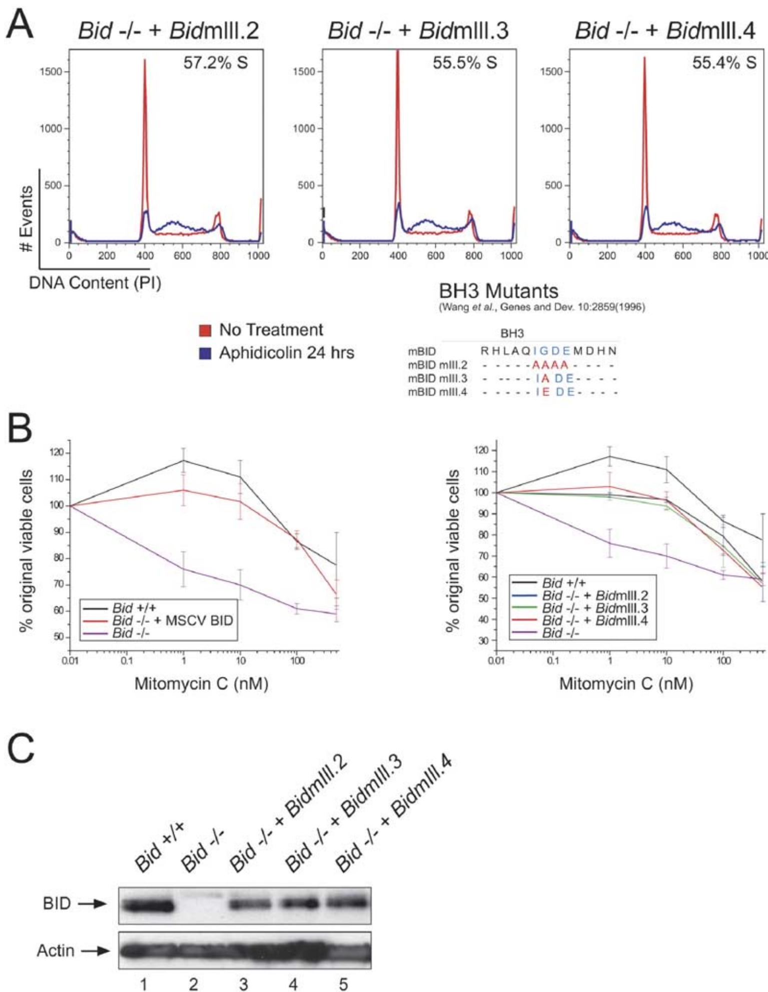

Figure 4. A Functional BID BH3 Domain Is Not Required to Restore S Phase Accumulation of *Bid*$^{-/-}$ MPCs Following Aphidicolin Treatment

(A) BID protein harboring apoptosis-inactivating mutations in the BH3 domain was introduced into *Bid*$^{-/-}$ MPCs by retroviral transduction. Cell cycle profiles were analyzed by PI staining following 18 hr of aphidicolin treatment.

(B) *Bid*$^{-/-}$ MPCs transduced either with wild-type BID or BID with the apoptosis-inactive BH3 domain mutations regain normal resistance to mitomycin c treatment. Viability following treatment with increasing doses of mitomycin c after 24 hr was monitored by Trypan blue exclusion.

(C) BID and BID BH3 mutants were expressed equally in the cell lines generated for use in this experiment as monitored by immunoblotting with anti-BID antisera.

Manke et al., 2003; O'Neill et al., 2000). BID has at least two ATM/ATR/DNA-PKcs consensus phosphorylation sites at residues S61 and S78 (Figure 6A), with S78 conserved between mouse and human BID. BID is phosphorylated in a dose-dependent manner at serines 61/64 and 78 as well as serine 61 following treatment with hydroxyurea, aphidicolin, and mitomycin c, all of which cause DNA damage via replicative stress (Figure 6B and Figure S6). BID is also phosphorylated following treatments with agents inducing DNA strand breaks such as etoposide, UV, and IR (Figure 6C). We used antibodies raised against phosphopeptides of the regions surrounding residues 61/64 (Desagher et al., 1999) and 61 and 78 (Dr. Atan Gross [Kamer et al., 2005, this issue of *Cell*] in collaboration with the Bethyl Laboratories, Inc., Montgomery, Texas), and confirmed the specificity of the phosphoantibodies using extracts from *Bid*$^{-/-}$ cells (Figure S6). The above data is consistent with constitutive phosphorylation of Bid on serine 64, with stimulation of phosphorylation on serine 61 in response to DNA damage. Thus, in response to DNA damage, BID is phosphorylated at the ATM/ATR/DNA-PKcs consensus sites, suggesting that its role in this pathway may be regulated by these DNA repair kinases.

BID Phosphorylation Is Inhibited by Wortmannin

Wortmannin is a fungal metabolite that inhibits the kinase activities of ATM, ATR, and DNA-PKcs (Sarkaria et al., 1998). BID phosphorylation in response to hydroxyurea treatment is decreased in the presence of levels of wortmannin known to inhibit ATM and DNA-PKcs, but only partially inhibit ATR (Figure 6D, lane 4 versus lane 6). Hydroxyurea-induced BID phosphorylation is not decreased in the presence of the PI3 kinase inhibitor LY294002 (Figure 6D, lane 5). Although LY294002 has been reported to inhibit DNA-PKcs, but not ATM or ATR (Stiff et al., 2004), significantly higher doses (200 μM) are required to produce minimal inhibition of hydroxyurea-induced Bid phosphorylation (Figure S7B). The above data are consistent with a minimal role for PI3 kinases in BID phosphorylation downstream of DNA damage and suggest that BID may be a substrate of one of the DNA-damage kinases.

Since the casein kinase family has been reported to phosphorylate BID, (Desagher et al., 1999), we also tested specific inhibitors of these kinases. Inhibitors of either casein kinase 1 (CKI-7) or casein kinase 2 (TBB) do not abolish hydroxyurea-induced phosphorylation of BID at serine 61 or 78 (Figure S7A, lanes 4 and 3, respectively, versus lane 2), suggesting that DNA dam-

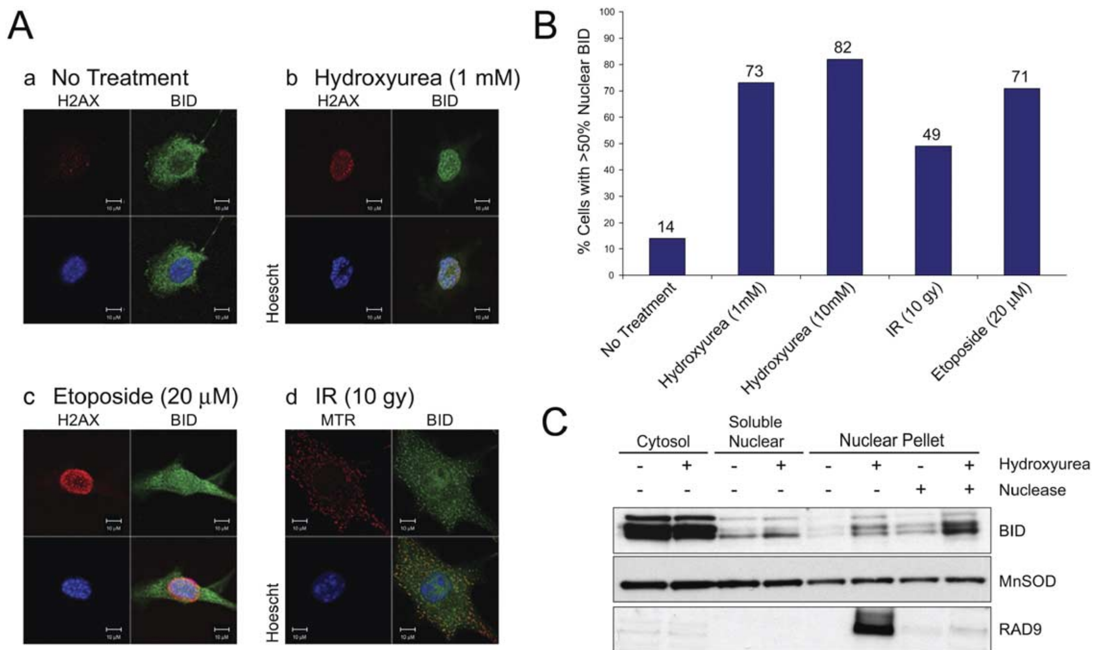

Figure 5. BID Translocates to the Nucleus Following DNA Damage

(A) Immunofluorescence confocal imaging of HA-tagged BID in mouse embryonic fibroblasts at 2 hr following (a) no treatment (b) hydroxyurea (1 mM), (c) etoposide (20 μM), and (d) Ionizing radiation (10 Gy).

(B) Percent of cells with >50% nuclear localization by confocal microscopy following 2 hr of treatment with DNA-damaging agents.

(C) Subcellular fractionation of MPCs at 2 hr following hydroxyurea treatment (1 mM). BID is found in the insoluble chromatin fraction following hydroxyurea.

age-induced BID phosphorylation may be mediated by a kinase distinct from the casein kinases.

BID Is a Substrate of ATM/ATR

To further elucidate the kinase responsible for regulation of BID phosphorylation, we evaluated a series of MEFs deficient for the DNA repair kinases ATM, ATR, and DNA-PKcs. In the absence of ATM, phosphorylation of BID at serines 61/64 and 78 in response to hydroxyurea, UV light, and ionizing radiation is nearly completely abrogated (Figure 6E, lanes 6, 7, and 8). In contrast, BID is phosphorylated at serines 61/64 and 78 in response to DNA damage induced by hydroxyurea and IR, even in cells partially deficient for ATR or deficient for DNA-PKcs (Figure 6H, lane 4, and Figure S8, lane 4). These data suggest that ATM is the major kinase mediating the phosphorylation of BID in response to IR, UV, and hydroxyurea-induced DNA damage. ATM has been reported to respond primarily to agents such as IR that generate double-strand breaks, while ATR appears to respond to agents inducing multiple types of DNA damage (Zhou and Elledge, 2000). ATM is activated by these types of damage under our conditions, as it is autophosphorylated on serine 1981 (Bakkenist and Kastan, 2003), and a downstream substrate of ATM, Chk2, is also activated (Figure 6F). Of note, we cannot rule out a role for ATR in BID phosphorylation as the Cre-mediated excision of ATR (Brown and Baltimore, 2003; Stiff et al., 2004), did not completely eliminate ATR expression (Figure 6H). In addition, accumulation of double-strand breaks in the resultant ATR-deficient cells may lead to activation of ATM kinase activity (Brown and Baltimore, 2003; Cha and Kleckner, 2002; Lopes et al., 2001) or activation of a compensatory kinase may result in nonspecific phosphorylation of BID. ATR is active in our ATM null MEFs, since the ATR substrate Chk1 is phosphorylated in response to the HU and UV treatment conditions used (Figure 6G). Interestingly, full-length CHK1 appears to be significantly decreased in myeloid cells, and we note the presence of a smaller form of CHK1, raising the possibility that the signaling pathway downstream of UV in myeloid cells may be distinct and may account for the similar UV sensitivity in *Bid*$^{-/-}$ and *Bid*$^{+/+}$ cells. Nevertheless, neither ATR nor DNA-PKcs compensates for the loss of ATM.

To determine if ATM and/or ATR could directly phosphorylate BID, we performed in vitro kinase assays using FLAG-tagged ATM and ATR and recombinant mouse BID. Wild-type but not kinase-inactive human ATM and ATR phosphorylate BID in vitro (Figure 6I, lanes 2 and 4 versus lanes 3 and 5), suggesting that BID can serve as a substrate of both ATM and ATR. Taken together with the above genetic studies, ATM or a kinase downstream of ATM is strongly implicated as the major kinase-mediating BID phosphorylation following DNA damage.

Bid$^{-/-}$ MPCs Have an Intra-S Phase Checkpoint Defect

To further dissect the cell cycle S phase aberration in *Bid*$^{-/-}$ MPCs, we tested the ability of these MPCs to

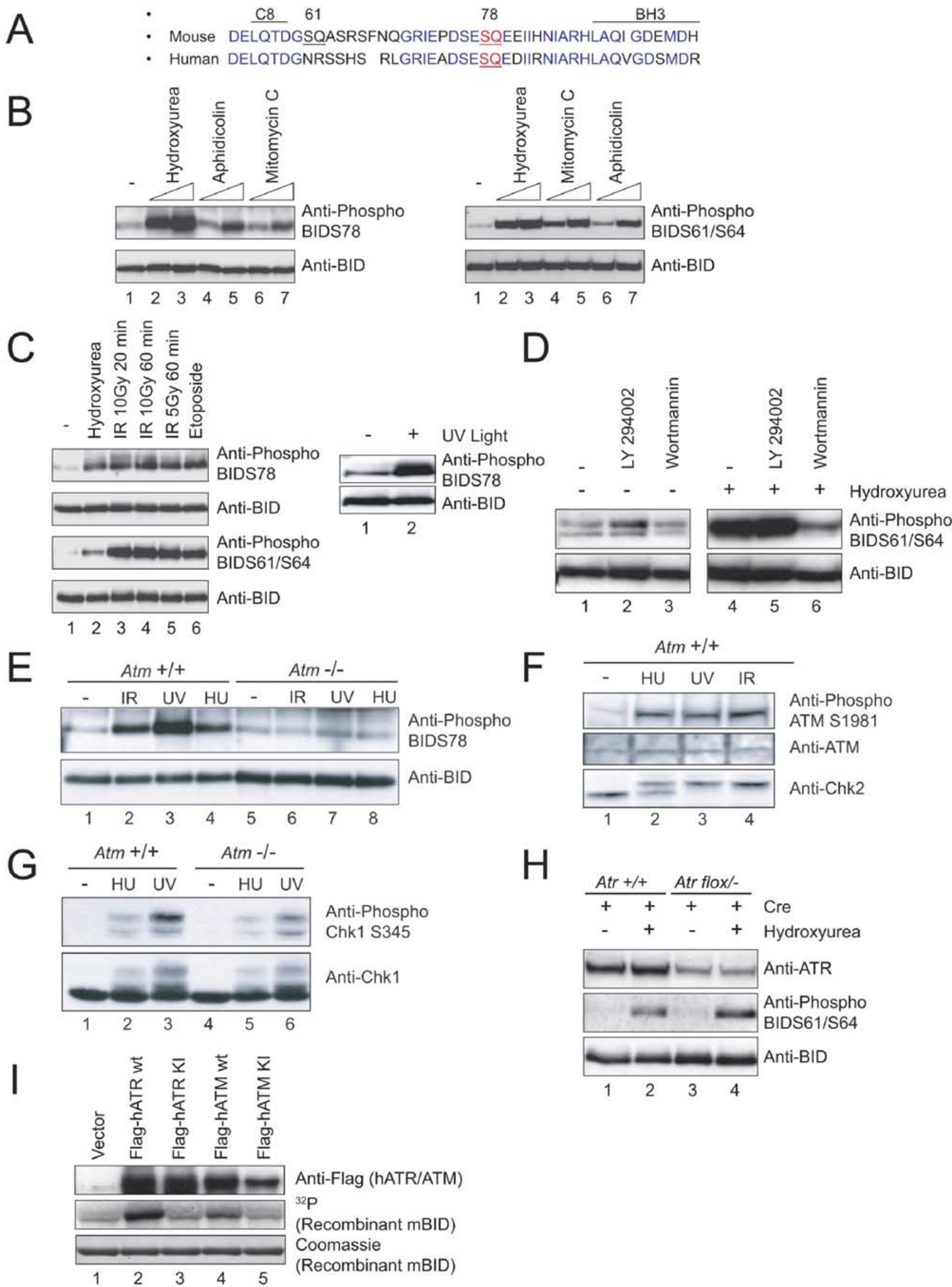

Figure 6. Bid Is a Substrate of ATM Downstream of DNA Damage

Similar results were obtained for residues 61/64 and 78 but for some panels only blots for either 61/64 or 78 are shown.

(A) Sequence alignment of mouse and human BID. Potential ATM/ATR consensus phosphorylation sites at serines 61and 78 are underlined. Serine residues conserved between mouse and human are indicated in red. The caspase 8 cleavage site (C8) and BH3 domain are indicated.

(B) BID is phosphorylated on serines 61 and 78 in a dose-dependent manner in response to hydroxyurea, aphidicolin, and mitomycin c treatment. Wild-type MPCs were incubated for 3 hr with 1 mM and 10 mM hydroxyurea, 1 μM and 10 μM aphidicolin, 1 μM and 10 μM (30 μM, or three times the previous dose, in right panel) mitomycin c. The cells were harvested and BID was immunoprecipitated, followed by immunoblotting with anti-phospho BIDS61/64 or anti-phospho BIDS78. The blots were then stripped and blotted for total BID levels.

(C) BID is phosphorylated on serines 61and 78 in response to treatment with hydroxyurea, IR, and etoposide. Wild-type MPCs were incubated for 3 hr either with 1 mM hydroxyurea, 10 μM etoposide, 10 J/m^2 UV light, or with 5 Gy or 10 Gy of ionizing radiation for the times indicated. To monitor BID phosphorylation, samples were subjected to BID immunoprecipitation and immunoblotting with anti-phospho BIDS61/64 or anti-phospho BIDS78 as in (B).

(D) Hydroxyurea-induced phosphorylation of BID is abolished on serine 61(and serine 78, see Figure S6) following treatment with wortmannin but not LY294002. Wild-type MPCs were pretreated with wortmannin (10 μM; Sigma) or LY 294002 (50 μM; Sigma) for 30 min prior to the addition of 10 mM hydroxyurea for 2 hr.

(E) DNA damage-induced phosphorylation of Bid is abolished in ATM null cells. wt or ATM-deficient MEFs were treated with 10 mM hydroxyurea for 2 hr, 10 Gy IR for 1 hr, or 10 J/m^2 UV for 2 hr. Cells were harvested and lysates were analyzed for Bid phosphorylation as in (B). SV40-transformed MEFs were used in the experiment shown, but similar results were seen using primary MEFs.

undergo replication arrest following treatment with either IR using a classic radioresistant DNA synthesis (RDS) assay, or modifying the RDS assay to assess replication arrest after treatment with mitomycin c. *Bid*$^{+/+}$ MPCs but not *Bid*$^{-/-}$ MPCs undergo replication arrest in response to both mitomycin c and IR treatment (Figures 7A and 7C, respectively). *Bid*$^{-/-}$-activated T cells (Figure 7D) display a similar abrogation of the IR-induced replication arrest, confirming that this intra-S phase checkpoint defect is a general feature of BID deficiency. Wild-type BID as well as BH3 mutant BID transduced into *Bid*$^{-/-}$ MPCs restored replication arrest following IR (Figure 7C, green and yellow bars, respectively), providing further evidence that the checkpoint defect is mediated by BID. Taken together, the above data provide strong evidence that BID plays a role in the intra-S phase checkpoint and that this role is mediated by a region of BID distinct from its prodeath domain.

The S Phase Role of BID Is Mediated by Phosphorylation at Position 78

Endogenous levels of BID S78A transduced into *Bid*$^{-/-}$ MPCs are unable to restore aphidicolin-induced S phase arrest (Figure 7B), suggesting that BID phosphorylation at serine 78 may function at the S phase checkpoint. In addition, *Bid*$^{-/-}$ MPCs transduced with a BID S78A mutant remain defective in IR-induced S phase arrest (Figure 7C, blue bar). *Bid*$^{-/-}$ MPCs transduced with the BID S61A mutant exhibit excessive apoptosis, consistent with the published report from Desagher et al. (1999) (data not shown). The cell cycle role of BID serine 61 in response to replicative stress will thus require additional study. The above results strongly suggest that BID's S phase role downstream of DNA damage is mediated by phosphorylation of the ATM/ATR consensus site at position 78.

Discussion

BID deficiency, a proximal defect in the death-receptor pathway, results in altered myeloid homeostasis. In the absence of BID, myeloid cells resist apoptosis, accumulate mutations, and display aspects of unchecked proliferation, culminating in a clonal malignancy of the myeloid lineage resembling human CMML (Zinkel et al., 2003). The surprising degree of genomic instability of these myeloid leukemias suggests a role for BID in preserving genomic integrity that places BID at an early point in the path to determine the fate of a cell. Here, we show that BID plays an unexpected role in the intra-S phase checkpoint downstream of DNA damage that is distinct from its proapoptotic role. ATM/ATR-mediated BID phosphorylation at serine 78 is required for the IR-mediated intra-S phase checkpoint. An intact BH3 domain, which is required for apoptosis, is not required for the BID-mediated S phase effects or the increased sensitivity to replicative stress, suggesting that the role of BID in the DNA-damage response is distinct from its proapoptotic function. Furthermore, like ATM and ATR (Dart et al., 2004; Gately et al., 1998), BID localizes to the chromatin fraction of the nucleus following treatment with DNA-damaging agents.

One interesting feature of *Bid*$^{-/-}$ myeloid cells is their apparent lack of sensitivity to IR or UV irradiation. Our data strongly suggest that ATM is a major upstream kinase of BID following DNA damage, indicating that this is an important signaling pathway. *Bid*-deficient hematopoietic cells display a profound defect in the intra-S phase checkpoint in response to IR, demonstrating a biological role for BID downstream of ATM signaling. Of note, there is precedence for important signaling pathways that do not result in a phenotype with respect to viability. For example, ATR mediates phosphorylation and monoubiquitination of Fanconi D2, (Andreassen et al., 2004) but fibroblasts deficient in FANCD2 do not display significantly increased sensitivity to UV (Kalb et al., 2004). Given the importance of apoptosis to maintenance of homeostasis in hematopoietic cells, it is possible that in the absence of BID, another BCL-2 family member compensates for the loss of BID's apoptotic function. Following IR treatment, BID is localized both in the mitochondria and in the nucleus. It is also intriguing to envision that both the proapoptotic function of BID and its role downstream of DNA damage may be operative simultaneously and that the fate of the cell to proliferate or to die may be balanced by these two functions.

Bid$^{-/-}$ myeloid progenitor cells have a phenotype resembling that found in cells with chromosomal instability syndromes such as Fanconi anemia, Bloom's syndrome, and the hereditary breast and ovarian cancer syndromes involving BRCA1. These phenotypes include the presence of tri- and quadriradial chromosomes, intra-S phase checkpoint defects, and hypersensitivity to DNA-damaging agents (D'Andrea, 2003;

(F) ATM is activated by DNA damage under the conditions used as indicated by immunoblotting with Anti-phosphoATMS1981. In addition, a downstream substrate of ATM, Chk2, is also activated by the DNA-damage treatments used. Chk2 phosphorylation is visualized by an upward shift in mobility using Anti-Chk2 antisera (BD Biosciences, monoclonal).

(G) ATR is active in the ATM$^{-/-}$ MEFs, however, does not compensate for the absence of ATM. ATR activity was assessed by monitoring phosphorylation of Chk1, a downstream substrate of ATR, in response to DNA damage. Chk1 phosphorylation on serine 345 was induced by DNA damage in both wt and ATM knockout MEFs. Chk1 phosphorylation also induces a mobility shift and was monitored using a Chk1 antibody (Santa Cruz, monoclonal).

(H) DNA damage-induced phosphorylation is not abolished in ATR flox/– cells. ATR was deleted using retrovirally introduced Cre recombinase. wt MEFs were also infected and used as a control. After 24 hr, cells were treated with 10 mM hydroxyurea for 2 hr and analyzed for Bid phosphorylation as in (B). Efficiency of ATR deletion was monitored by immunoblotting using anti-ATR antisera (Serotec).

(I) Bid is a substrate for ATM and ATR in vitro. FLAG-tagged hATR or hATM or FLAG-tagged kinase-inactive hATR or hATM was overexpressed in 293T cells, immunoprecipitated with anti-FLAG M2 agarose, washed several times, and then incubated in the presence of recombinant mBID and γ^{32}PATP. Reactions were separated on 12% SDS-PAGE, and phosphorylated Bid was visualized by autoradiography. Levels of FLAG-ATM and FLAG-ATR were monitored by immunoblotting with anti-FLAG M2 antisera and levels and purity of recombinant mBid were visualized by Coomassie staining.

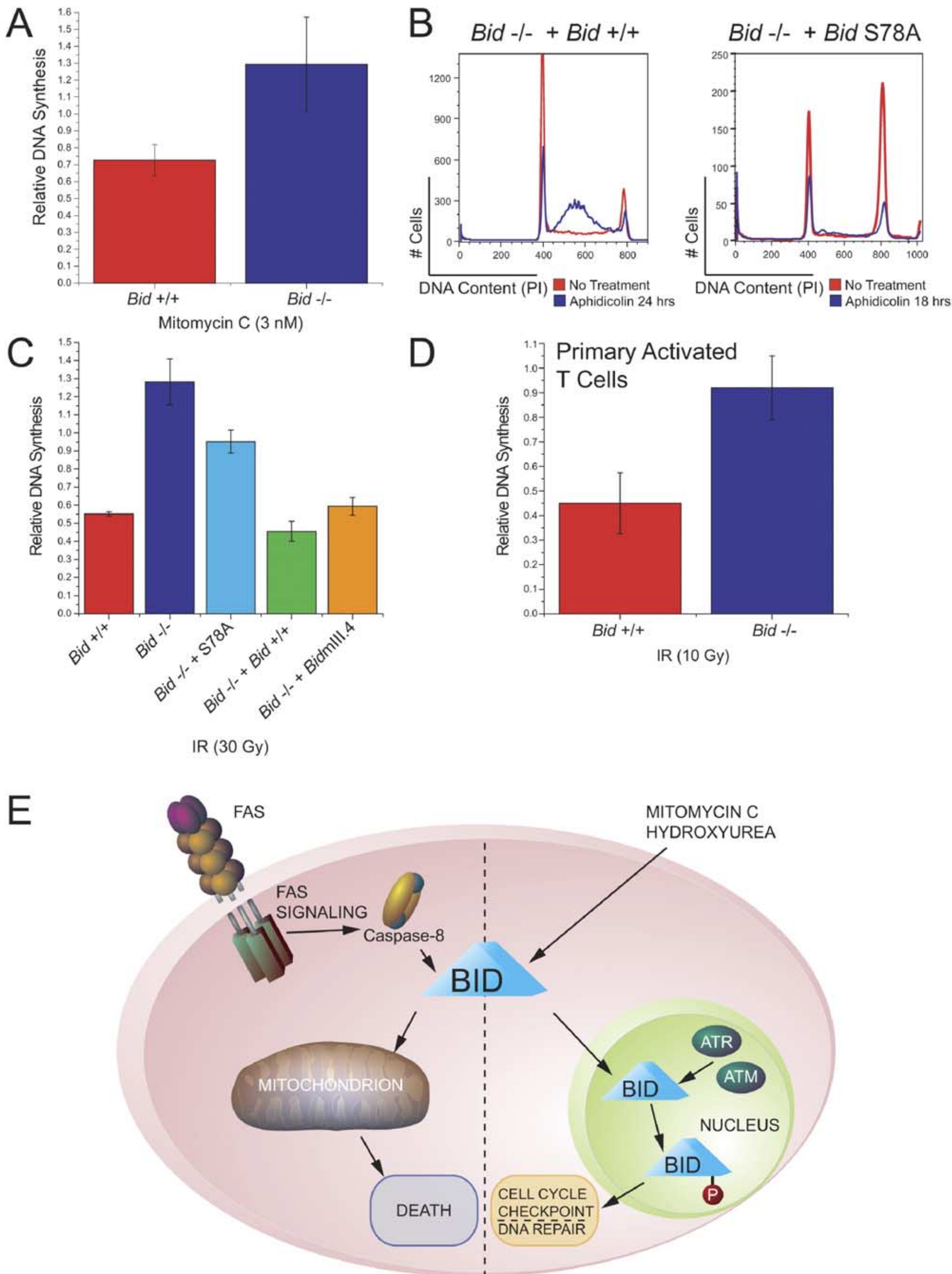

Figure 7. BID Phosphorylation Is Linked to Maintenance of the S Phase Checkpoint

(A) *Bid*$^{-/-}$ MPCs display an S phase checkpoint defect following mitomycin c treatment. *Bid*$^{+/+}$ and *Bid*$^{-/-}$ MPCs were labeled for 24 hr with ^{14}C thymidine, treated with 3 μM mitomycin c for 4 hr, and incubated with ^{3}H thymidine for 30 min. The ratio of ^{3}H thymidine to ^{14}C thymidine was normalized to the appropriate untreated control to determine the relative amount of DNA synthesis. The error bars in (A), (C), and (D) represent the standard deviation of data points from three independent experiments.

(B) *Bid*$^{-/-}$ MPCs expressing the BID S78A mutant fail to restore S phase accumulation in BID null MPCs following aphidicolin treatment. *Bid*$^{-/-}$ MPCs into which either wild-type BID or BID S78A was introduced by retroviral transduction were incubated with 0.1 μM aphidicolin for 18–24 hr and DNA content was analyzed by PI staining and flow cytometry.

(C) *Bid*$^{-/-}$ MPCs expressing wild-type BID or the BH3 mutant BIDmIII.4 display an intact intra-S phase checkpoint following IR, whereas *Bid*$^{-/-}$ MPCs as well as *Bid*$^{-/-}$ MPCs expressing the BID S78A mutant display a defective intra-S phase checkpoint following IR treatment. Cells were labeled as above. The ratio of ^{3}H thymidine to ^{14}C thymidine was normalized to the appropriate untreated control to determine the relative amount of DNA synthesis.

(D) *Bid*$^{-/-}$ primary activated T cells display a defective intra-S phase checkpoint following IR treatment. Cells were labeled and analyzed as in (C).

(E) Model for dual roles of BID. Following death-receptor-induced apoptotic signals, BID is posttranslationally modified by caspase cleavage and myristoylation and translocates to the mitochondrion to activate the downstream apoptotic program. BID has a distinct role downstream of DNA damage. Following treatment with agents inducing DNA damage such as mitomycin c, IR, and hydroxyurea, BID accumulates in the nucleus and is phosphorylated by the DNA-damage kinase ATM. This phosphorylation is required for a downstream function in cell cycle checkpoint control.

Langland et al., 2002; Scully and Livingston, 2000; Wu et al., 2001). The defective proteins in these syndromes have been shown to play a role in the repair of DNA damage. These similarities in phenotype warrant future studies to determine if BID may play a role in DNA repair.

How might BID exert its effect in response to DNA damage? The cell cycle checkpoint machinery is localized in the nucleus in multiprotein complexes. The location of BID in the nucleus following DNA damage as well as its functional interaction with ATM/ATR suggest that BID could be a member of such a multiprotein complex. The amino acid sequence of BID does not have any obvious nuclear localization signals, suggesting that BID is transported into the nucleus as part of a protein complex that moves in response to DNA damage. BID may play a role to stabilize the complex or it may help orient members of the complex in order to facilitate subsequent enzymatic steps. Finally, it is possible that BID may possess an additional enzymatic function integral to checkpoint execution.

BID is phosphorylated following DNA damage in fibroblasts and hematopoietic cells. The intra-S phase checkpoint, important for maintaining genomic stability, is mediated by BID phosphorylation. Yet in vivo, *Bid* deficiency manifests as altered homeostasis and leukemogenesis with considerable genomic instability, specifically in the myeloid lineage. Hematopoietic cells are particularly sensitive to low to moderate levels of genotoxic stress relative to other cell types, relying on apoptosis to prevent accumulation of mutations. Following DNA damage, cells initiate a complex series of responses, including the activation of checkpoints or triggering apoptosis. In order to maintain homeostasis, these pathways must be carefully balanced and coordinated in the hematopoietic lineage. BID, with its dual function in both apoptosis and the intra-S phase checkpoint, is well positioned to serve as a mediator between these two pathways.

Experimental Procedures

Cell Lines

Hox11 immortalization of MPCs was as follows: after sacrifice by CO_2 asphyxiation, bone marrows were harvested from six $Bid^{-/-}$ mice (generation F9 on a C57Bl6 background) as well as 6 age and sex-matched wild-type mice. MPCs were isolated by lineage depletion (Lin: CD3, Gr-1, B220, ter119) followed by positive selection of Sca-1$^+$ cells by magnetic beads (Miltenyi). These cells were cocultured with irradiated (30 Gy) 90% to 100% confluent NIH 3T3 hph-HOX11 retroviral producer cells in infection medium (IMDM, 20% fetal calf serum [FCS] 100 U/ml penicillin-streptomycin, 2 mM glutamine, 10 ng/ml IL-3, 20 ng/ml stem cell factor [SCF], 10 ng/ml granulocyte-macrophage colony stimulating factor [GM-CSF], and 2 ng/ml granulocyte colony stimulating factor [G-CSF]) for 3 days at 37°C in 5% CO_2 (Hawley et al., 1994). The cells growing in suspension were expanded in IMDM 20% FCS, 100 U/ml penicillin-streptomycin, 2 mM glutamine with 10% conditioned medium from WEHI cells as a source of IL-3. Cells were immortalized on two separate occasions. Cells from these two separate preparations behave similarly, and data from the two preparations have been pooled for presentation.

ATR was deleted from ATR flox/– and control MEFs using retroviral transduction with pMIG-CRE-GFP and ATR levels verified by immunoblotting. DNA-PKcs$^{-/-}$ and control MEFs were cultured using standard methods. ATM (129S6/SvEvTac-Atm^{tm1Awb}/J) mice (Jackson Laboratory) were used to prepare MEFs by routine methods.

Cell Death Assays

Hox11-immortalized MPCs were treated with a range of doses of hydroxyurea (10 μM–1 mM), mitomycin c (1 nM–1.5 μM), aphidicolin, IR (1 Gy–10 Gy), etoposide (0.2 μM–100 μM) and UV (2–100 J/M^2). Cell viability was measured after 24 hr by Trypan blue staining.

MPCs were isolated by lineage depletion followed by positive selection of Sca-1$^+$ cells by magnetic beads (Miltenyi). Cells were cultured in IMDM, 20% fetal calf serum (FCS), 100 U/ml penicillin-streptomycin, 2 mM glutamine, 10 ng/ml IL-3, 20 ng/ml stem cell factor (SCF), 10 ng/ml GM-CSF, and 2 ng/ml G-CSF for 3 days at 37°C in 5% CO_2 and then treated with DNA-damaging agents as above.

Populations enriched in primary peripheral CD8$^+$ T cells were obtained from $Bid^{-/-}$ mice, which have been bred into an H-Y T cell receptor transgenic mouse model (Kisielow et al., 1988). After sacrifice by CO_2 asphyxiation, spleens were harvested from $Bid^{-/-}$ as well as $Bid^{+/+}$ mice; splenocytes were isolated and incubated in RPMI + IL-2 + 0.1 μM antigenic peptide (HY) for 3 days and treated with mitomycin c and hydroxyurea, and cell viability was measured after 24 hr as above.

Metaphase Spreads

$Bid^{+/+}$ and $Bid^{-/-}$ MPCs were treated with 100 μM mitomycin c for 24 hr. Cells were fixed and metaphase spreads prepared by standard methods. Fifty metaphases each from $Bid^{+/+}$ and from $Bid^{-/-}$ MPCs were scored for chromosomal damage per metaphase as follows: each chromosome break was given a score of +1, and each triradial or quadriradial form was given a score of +2

Cell Cycle Analysis

One million cells were resuspended in 200 μl Krishan's reagent (0.1% NaCitrate, 0.03% NP40, 0.05 mg/ml propidium iodide, 0.02 mg/ml RNase A), incubated for 15 min at room temperature (RT) in the dark, and analyzed on a Becton-Dickenson FACS machine using FloJo analysis software.

BrDU analysis was as follows: cells were incubated with 10 μM BrDU for 45 min, washed, and incubated with 100 mM hydroxyurea or 0.1 μM aphidicolin. S phase cells were followed by FACS analysis of BrDU$^+$ cells at the indicated times using the BrDU flow kit (BD Pharmingen) according to the manufacturer's instructions.

Antibodies and Recombinant Proteins

Antibodies were as follows: anti-BID rabbit polyclonal 1:1000 (Wang et al., 1996), anti-BID rabbit polyclonal (Santa Cruz), anti-ATR rabbit polyclonal 1:1000 (Serotec), anti-phospho BidS61/64 BID rabbit polyclonal 1:500, a kind gift from Drs. Desagher and Martinou (Desagher et al., 1999); anti-phospho BidS78 BID and anti-phospho BidS61, rabbit polyclonals, 1:500 (Dr. Atan Gross in collaboration with Bethyl Laboratories, Inc., Montgomery, Texas); anti-phospho ATMS1981 1:500 (Rockland), anti-phospho Chk1S345 1:500 (Cell Signaling), Anti-Chk1 1:500 (Santa Cruz), and Anti-Chk2 1:250 (BD Biosciences); anti-MnSOD 1:1000 (Stressgen), and anti-RAD9 1:250 (Santa Cruz).

S61A BID and S78A BID were obtained using the Quickchange XL site-directed mutagenesis kit (Stratagene) and cloned into the BamHI and EcoRI sites of the pBABE retroviral expression vector, and the NotI/XhoI sites of pOZ-FH-N vector. BIDmIII.2, BIDmIII.3, and BIDmIII.4 were amplified by PCR from pCDNA3 harboring these constructs (Wang et al., 1996) and cloned into the BamHI/EcoRI sites of pBABE puro.

Epitope-tagged BID was generated by cloning the cDNA for BID into pOZ-FH-C (Nakatani and Ogryzko, 2003) to generate BID that is tagged at the C terminus with FLAG and HA.

Immunofluorescence

BID-transduced MEFs were treated with DNA-damaging agents (IR [10 Gy], HU [1mM, 10 mM], Etoposide [20 μM, 100 μM]) and fixed with methanol:acetone 3:1. Primary antibodies used were Alexafluor 488-conjugated anti-HA (Molecular Probes), and anti-phospho-H2AX (Upstate). Texas red-conjugated goat anti-rabbit secondary antibody (Molecular Probes) was used. Where indicated, cells were incubated for 1 hr with mitotracker red prior to fixation

and staining. Staining was visualized using a Zeiss confocal microscope.

Retroviral Transduction

Retroviral supernatants were generated by transient transfection of the ecotropic packaging cell line 293T with the appropriate expression plasmid. Tagged BID was introduced into *Bid*$^{-/-}$ MEFs or MPCs by retroviral transduction. MPCs were infected by spin inoculation and cells were selected in puromycin.

In Vitro Kinase Assays

293T cells were transiently transfected with pCDNA3-FLAG ATR WT or kinase inactive (KI) (K2327R) (Tibbetts et al., 1999) or pCDNA3-FLAG-ATM WT or KI (Canman et al., 1998) or pCDNA3 vector alone using Fugene 6 reagent. In vitro kinase assays were performed using standard methods (details in the Supplemental Experimental Procedures).

Bid Immunoprecipitations

MPCs or MEFs were lysed in TNE buffer, and endogenous mouse Bid was immunoprecipitated with biotinylated anti-Bid antibody. Immunoprecipitates were separated on 12% SDS-PAGE and the phosphorylation status of Bid was monitored using phosphospecific antisera recognizing S61/64, S61, or S78. Total Bid levels were monitored using an Anti-Bid antibody .

Kinase Inhibitor Treatments

Cells were pretreated with wortmannin (Sigma), LY 294002 (Sigma) (Vlahos et al., 1994), casein kinase 1 inhibitor CKI-7 (N-[2-aminoethyl]-5-chloro-isoquinoline-8-sulfonamide) (US Biological) (Chijiwa et al., 1989) or casein kinase 2 inhibitor TBB (4,5,6,7-Tetrabromobenzotriazole) (Calbiochem) (Loizou et al., 2004; Sarno et al., 2001, 2002) for 30 min prior to the addition of 10 mM hydroxyurea for 2 hr. Inhibitor concentrations are indicated in the figure legends.

DNA-Damaging Agents

Cells were treated with hydroxyurea (Sigma), mitomycin c (Sigma), aphidicolin (Sigma), and etoposide (Sigma) as indicated in the figure legends. Cells were irradiated using a Gammacell 40 or Gammacell 100 Cesium 137 source for the doses and times indicated in the figure legends. Cells were UV irradiated with 10 J/m^2 of UV using a UV Stratalinker 2400 (Stratagene) and harvested following 2 hr of incubation.

Subcellular Fractionation

Subcellular fractionation was performed using a modified Dgnam protocol. For details, see the Supplemental Experimental Procedures.

Supplemental Data

Supplemental Data include nine figures and Supplemental Experimental Procedures and can be found with this article online at http://www.cell.com/cgi/content/full/122/4/579/DC1/.

Acknowledgments

We thank Dr. Steve Elledge for critical reading of the manuscript. We thank Eric Smith for preparing the figures, and Dr. Connie Gee and Eric Smith for editing. We thank Drs. David Livingston, Dan Silver, Roger Greenberg, Yoshihiro Nakatani, and Ralph Scully for helpful discussions. We thank Dr. Joon Oh for preparing the recombinant BID for use in kinase assays, Dr. Charles Lee of the Dana-Farber/Harvard Cancer Center (DF/HCC) Cytogenetics Core for review of the metaphase spreads, and Matthew Salanga of the Imaging Core Facility, Division of Neuroscience, Children's Hospital for confocal microscopy. ATR flox/– and control MEFs, DNA-PKcs$^{-/-}$ and control MEFs, ATM wt and KI cDNA, ATR wt and KI cDNA, and anti-phospho 61/64 BID were kind gifts from from Eric Brown (University of Pennsylvania), Guillermo Taccioli (Boston University Medical Center), Michael Kastan (St. Jude's Cancer Center), Robert Abraham (The Burnham Institute), Solange Desagher, and Jean-Claude Martinou, respectively. S.S.Z. is supported by NCI Mentored Clinical Scientist Award CA098394 and a V Foundation Scholar Award; K.E.H. is supported by a Leukemia and Lymphoma Society Fellow Award. This work is supported in part by NIH grants P01 CA92625 and R37 CA50239. S.J.K. is an investigator of the Howard Hughes Medical Institute.

Received: December 31, 2004
Revised: May 12, 2005
Accepted: June 13, 2005
Published: August 25, 2005

References

Andegeko, Y., Moyal, L., Mittelman, L., Tsarfaty, I., Shiloh, Y., and Rotman, G. (2001). Nuclear retention of ATM at sites of DNA double strand breaks. J. Biol. Chem. *276*, 38224–38230.

Andreassen, P.R., D'Andrea, A.D., and Taniguchi, T. (2004). ATR couples FANCD2 monoubiquitination to the DNA-damage response. Genes Dev. *18*, 1958–1963.

Bakkenist, C.J., and Kastan, M.B. (2003). DNA damage activates ATM through intermolecular autophosphorylation and dimer dissociation. Nature *421*, 499–506.

Banin, S., Moyal, L., Shieh, S., Taya, Y., Anderson, C.W., Chessa, L., Smorodinsky, N.I., Prives, C., Reiss, Y., Shiloh, Y., and Ziv, Y. (1998). Enhanced phosphorylation of p53 by ATM in response to DNA damage. Science *281*, 1674–1677.

Baus, F., Gire, V., Fisher, D., Piette, J., and Dulic, V. (2003). Permanent cell cycle exit in G2 phase after DNA damage in normal human fibroblasts. EMBO J. *22*, 3992–4002.

Brown, E.J., and Baltimore, D. (2003). Essential and dispensable roles of ATR in cell cycle arrest and genome maintenance. Genes Dev. *17*, 615–628.

Canman, C.E., Lim, D.S., Cimprich, K.A., Taya, Y., Tamai, K., Sakaguchi, K., Appella, E., Kastan, M.B., and Siliciano, J.D. (1998). Activation of the ATM kinase by ionizing radiation and phosphorylation of p53. Science *281*, 1677–1679.

Cha, R.S., and Kleckner, N. (2002). ATR homolog Mec1 promotes fork progression, thus averting breaks in replication slow zones. Science *297*, 602–606.

Chijiwa, T., Hagiwara, M., and Hidaka, H. (1989). A newly synthesized selective casein kinase I inhibitor, N-(2-aminoethyl)-5-chloroisoquinoline-8-sulfonamide, and affinity purification of casein kinase I from bovine testis. J. Biol. Chem. *264*, 4924–4927.

Cliby, W.A., Roberts, C.J., Cimprich, K.A., Stringer, C.M., Lamb, J.R., Schreiber, S.L., and Friend, S.H. (1998). Overexpression of a kinase-inactive ATR protein causes sensitivity to DNA-damaging agents and defects in cell cycle checkpoints. EMBO J. *17*, 159–169.

D'Andrea, A.D. (2003). The Fanconi road to cancer. Genes Dev. *17*, 1933–1936.

Danial, N.N., and Korsmeyer, S.J. (2004). Cell death: Critical control points. Cell *116*, 205–219.

Dart, D.A., Adams, K.E., Akerman, I., and Lakin, N.D. (2004). Recruitment of the cell cycle checkpoint kinase ATR to chromatin during S phase. J. Biol. Chem. *279*, 16433–16440.

Desagher, S., Osen-Sand, A., Nichols, A., Eskes, R., Montessuit, S., Lauper, S., Maundrell, K., Antonsson, B., and Martinou, J.C. (1999). Bid-induced conformational change of Bax is responsible for mitochondrial cytochrome c release during apoptosis. J. Cell Biol. *144*, 891–901.

Di Leonardo, A., Linke, S.P., Clarkin, K., and Wahl, G.M. (1994). DNA damage triggers a prolonged p53-dependent G1 arrest and long-term induction of Cip1 in normal human fibroblasts. Genes Dev. *8*, 2540–2551.

Frei, C., and Gasser, S.M. (2000). RecQ-like helicases: the DNA replication checkpoint connection. J. Cell Sci. *113*, 2641–2646.

Gately, D.P., Hittle, J.C., Chan, G.K., and Yen, T.J. (1998). Characterization of ATM expression, localization, and associated DNA-dependent protein kinase activity. Mol. Biol. Cell *9*, 2361–2374.

Guo, Z., Kumagai, A., Wang, S.X., and Dunphy, W.G. (2000).

Requirement for Atr in phosphorylation of Chk1 and cell cycle regulation in response to DNA replication blocks and UV-damaged DNA in Xenopus egg extracts. Genes Dev. *14*, 2745–2756.

Hawley, R.G., Fong, A.Z., Lu, M., and Hawley, T.S. (1994). The HOX11 homeobox-containing gene of human leukemia immortalizes murine hematopoietic precursors. Oncogene *9*, 1–12.

Jacks, T., and Weinberg, R.A. (2002). Taking the study of cancer cell survival to a new dimension. Cell *111*, 923–925.

Kalb, R., Duerr, M., Wagner, M., Herterich, S., Gross, M., Digweed, M., Joenje, H., Hoehn, H., and Schindler, D. (2004). Lack of sensitivity of primary Fanconi's anemia fibroblasts to UV and ionizing radiation. Radiat. Res. *161*, 318–325.

Kamer, I., Sarig, R., Zaltsman, Y., Niv, H., Oberkovitz, G., Regev, L., Haimovich, G., Lerenthal, Y., Marcellus, R.C., and Gross, A. (2005). Proapoptotic BID is an ATM effector in the DNA-damage response. Cell *122*, this issue, 593–603.

Kim, S.T., Lim, D.S., Canman, C.E., and Kastan, M.B. (1999). Substrate specificities and identification of putative substrates of ATM kinase family members. J. Biol. Chem. *274*, 37538–37543.

Kisielow, P., Bluthmann, H., Staerz, U.D., Steinmetz, M., and von Boehmer, H. (1988). Tolerance in T-cell-receptor transgenic mice involves deletion of nonmature CD4+8+ thymocytes. Nature *333*, 742–746.

Langland, G., Elliott, J., Li, Y., Creaney, J., Dixon, K., and Groden, J. (2002). The BLM helicase is necessary for normal DNA double-strand break repair. Cancer Res. *62*, 2766–2770.

Loizou, J.I., El-Khamisy, S.F., Zlatanou, A., Moore, D.J., Chan, D.W., Qin, J., Sarno, S., Meggio, F., Pinna, L.A., and Caldecott, K.W. (2004). The protein kinase CK2 facilitates repair of chromosomal DNA single-strand breaks. Cell *117*, 17–28.

Lopes, M., Cotta-Ramusino, C., Pellicioli, A., Liberi, G., Plevani, P., Muzi-Falconi, M., Newlon, C.S., and Foiani, M. (2001). The DNA replication checkpoint response stabilizes stalled replication forks. Nature *412*, 557–561.

Manke, I.A., Lowery, D.M., Nguyen, A., and Yaffe, M.B. (2003). BRCT repeats as phosphopeptide-binding modules involved in protein targeting. Science *302*, 636–639.

Nakatani, Y., and Ogryzko, V. (2003). Immunoaffinity purification of mammalian protein complexes. Methods Enzymol. *370*, 430–444.

Nyberg, K.A., Michelson, R.J., Putnam, C.W., and Weinert, T.A. (2002). Toward maintaining the genome: DNA damage and replication checkpoints. Annu. Rev. Genet. *36*, 617–656.

O'Neill, T., Dwyer, A.J., Ziv, Y., Chan, D.W., Lees-Miller, S.P., Abraham, R.H., Lai, J.H., Hill, D., Shiloh, Y., Cantley, L.C., and Rathbun, G.A. (2000). Utilization of oriented peptide libraries to identify substrate motifs selected by ATM. J. Biol. Chem. *275*, 22719–22727.

Sancar, A., Lindsey-Boltz, L.A., Unsal-Kaccmaz, K., and Linn, S. (2004). Molecular mechanisms of mammalian DNA repair and the DNA damage checkpoints. Annu. Rev. Biochem. *73*, 39–85.

Sarkaria, J.N., Tibbetts, R.S., Busby, E.C., Kennedy, A.P., Hill, D.E., and Abraham, R.T. (1998). Inhibition of phosphoinositide 3-kinase related kinases by the radiosensitizing agent wortmannin. Cancer Res. *58*, 4375–4382.

Sarno, S., Reddy, H., Meggio, F., Ruzzene, M., Davies, S.P., Donella-Deana, A., Shugar, D., and Pinna, L.A. (2001). Selectivity of 4,5,6,7-tetrabromobenzotriazole, an ATP site-directed inhibitor of protein kinase CK2 ('casein kinase-2′). FEBS Lett. *496*, 44–48.

Sarno, S., Moro, S., Meggio, F., Zagotto, G., Dal Ben, D., Ghisellini, P., Battistutta, R., Zanotti, G., and Pinna, L.A. (2002). Toward the rational design of protein kinase casein kinase-2 inhibitors. Pharmacol. Ther. *93*, 159–168.

Sax, J.K., Fei, P., Murphy, M.E., Bernhard, E., Korsmeyer, S.J., and El-Deiry, W.S. (2002). BID regulation by p53 contributes to chemosensitivity. Nat. Cell Biol. *4*, 842–849.

Scaffidi, C., Fulda, S., Srinivasan, A., Friesen, C., Li, F., Tomaselli, K.J., Debatin, K.M., Krammer, P.H., and Peter, M.E. (1998). Two CD95 (APO-1/Fas) signaling pathways. EMBO J. *17*, 1675–1687.

Scully, R., and Livingston, D.M. (2000). In search of the tumour-suppressor functions of BRCA1 and BRCA2. Nature *408*, 429–432.

Scully, R., Puget, N., and Vlasakova, K. (2000). DNA polymerase stalling, sister chromatid recombination and the BRCA genes. Oncogene *19*, 6176–6183.

Shibue, T., Takeda, K., Oda, E., Tanaka, H., Murasawa, H., Takaoka, A., Morishita, Y., Akira, S., Taniguchi, T., and Tanaka, N. (2003). Integral role of Noxa in p53-mediated apoptotic response. Genes Dev. *17*, 2233–2238.

Stewart, E., Chapman, C.R., Al-Khodairy, F., Carr, A.M., and Enoch, T. (1997). rqh1+, a fission yeast gene related to the Bloom's and Werner's syndrome genes, is required for reversible S phase arrest. EMBO J. *16*, 2682–2692.

Stiff, T., O'Driscoll, M., Rief, N., Iwabuchi, K., Lobrich, M., and Jeggo, P.A. (2004). ATM and DNA-PK function redundantly to phosphorylate H2AX after exposure to ionizing radiation. Cancer Res. *64*, 2390–2396.

Tibbetts, R.S., Brumbaugh, K.M., Williams, J.M., Sarkaria, J.N., Cliby, W.A., Shieh, S.Y., Taya, Y., Prives, C., and Abraham, R.T. (1999). A role for ATR in the DNA damage-induced phosphorylation of p53. Genes Dev. *13*, 152–157.

Tibbetts, R.S., Cortez, D., Brumbaugh, K.M., Scully, R., Livingston, D., Elledge, S.J., and Abraham, R.T. (2000). Functional interactions between BRCA1 and the checkpoint kinase ATR during genotoxic stress. Genes Dev. *14*, 2989–3002.

Villunger, A., Michalak, E.M., Coultas, L., Mullauer, F., Bock, G., Ausserlechner, M.J., Adams, J.M., and Strasser, A. (2003). p53- and drug-induced apoptotic responses mediated by BH3-only proteins puma and noxa. Science *302*, 1036–1038.

Vlahos, C.J., Matter, W.F., Hui, K.Y., and Brown, R.F. (1994). A specific inhibitor of phosphatidylinositol 3-kinase, 2-(4-morpholinyl)-8-phenyl-4H–1-benzopyran-4-one (LY294002). J. Biol. Chem. *269*, 5241–5248.

Wang, K., Yin, X.M., Chao, D.T., Milliman, C.L., and Korsmeyer, S.J. (1996). BID: a novel BH3 domain-only death agonist. Genes Dev. *10*, 2859–2869.

Wei, M.C., Zong, W.X., Cheng, E.H., Lindsten, T., Panoutsakopoulou, V., Ross, A.J., Roth, K.A., MacGregor, G.R., Thompson, C.B., and Korsmeyer, S.J. (2001). Proapoptotic BAX and BAK: a requisite gateway to mitochondrial dysfunction and death. Science *292*, 727–730.

Wu, L., Davies, S.L., Levitt, N.C., and Hickson, I.D. (2001). Potential role for the BLM helicase in recombinational repair via a conserved interaction with RAD51. J. Biol. Chem. *276*, 19375–19381.

Yin, X.M., Wang, K., Gross, A., Zhao, Y., Zinkel, S., Klocke, B., Roth, K.A., and Korsmeyer, S.J. (1999). Bid-deficient mice are resistant to Fas-induced hepatocellular apoptosis. Nature *400*, 886–891.

Zha, J., Weiler, S., Oh, K.J., Wei, M.C., and Korsmeyer, S.J. (2000). Posttranslational N-myristoylation of BID as a molecular switch for targeting mitochondria and apoptosis. Science *290*, 1761–1765.

Zhou, B.B., and Elledge, S.J. (2000). The DNA damage response: putting checkpoints in perspective. Nature *408*, 433–439.

Zinkel, S.S., Ong, C.C., Ferguson, D.O., Iwasaki, H., Akashi, K., Bronson, R.T., Kutok, J.L., Alt, F.W., and Korsmeyer, S.J. (2003). Proapoptotic BID is required for myeloid homeostasis and tumor suppression. Genes Dev. *17*, 229–239.